Sciencexpress Reports

Global Anisotropies in TeV Cosmic Rays Related to the Sun's Local Galactic Environment from IBEX

N. A. Schwadron,[1,2]* F. C. Adams,[3] E. R. Christian,[4] P. Desiati,[5] P. Frisch,[6] H. O. Funsten,[7] J. R. Jokipii,[8] D. J. McComas,[2,9] E. Moebius,[1] G.P. Zank[10]

[1]University of New Hampshire, Space Science Center, Durham, NH 03824, USA. [2]Southwest Research Institute, San Antonio, TX 78228, USA. [3]University of Michigan, Physics Department, Ann Arbor, MI 48109, USA. [4]Goddard Space Flight Center, Greenbelt, MD 20771, USA. [5]University of Wisconsin, IceCube Observatory and Astronomy Department, Madison, WI 53706, USA.[6]University of Chicago, Department of Astronomy and Astrophysics, Chicago, IL 60637, USA. [7]Los Alamos National Laboratory, Space Science and Applications, Los Alamos, NM 87545, USA. [8]University of Arizona, Department of Planetary Sciences, Tucson, AZ 85721, USA. [9]University of Texas at San Antonio, San Antonio, TX 78249, USA. [10]University of Alabama, Huntsville, AL 35805, USA.

*Corresponding author. E-mail: n.schwadron@unh.edu

Observations with the Interstellar Boundary Explorer (IBEX) have shown enhanced energetic neutral atom (ENA) emission from a narrow, circular ribbon likely centered on the direction of the local interstellar medium (LISM) magnetic field. Here we show that recent determinations of the local interstellar velocity, based on interstellar atom measurements with IBEX, are consistent with the interstellar modulation of high energy (TeV) cosmic rays and diffusive propagation from supernova sources revealed in global anisotropy maps of ground-based high-energy cosmic-ray observatories (Milagro, Asγ and IceCube). Establishing a consistent local interstellar magnetic field direction using IBEX ENAs at hundreds to thousands of eV and galactic cosmic rays at tens of TeV has wide-ranging implications for the structure of our heliosphere and its interactions with the local interstellar medium, particularly important at the time when the Voyager spacecraft are leaving our heliosphere.

The heliosphere—the region surrounding our solar system that is carved out by the supersonic solar wind—moves through the local interstellar cloud (LIC), which is the part of the galactic environment surrounding the Sun. The heliosphere deflects much of the harmful cosmic ray radiation from the local galactic environment, thereby regulating the radiation environment throughout the solar system, which likely has important implications for Earth's atmosphere and life (*1*). IBEX recently provided updated values for the velocity vector of the heliosphere through the LIC (*2*) and direction for the local interstellar medium (LISM) magnetic field (Table 1 and Fig. 1) from the center of the IBEX ribbon of Energetic Neutral Atom (ENA) emission (*3–9*). These results show that the interstellar flow, after removing the motion of the Sun through the local standard of rest (LSR), is nearly perpendicular (87.6°± 3.0°) to the LISM magnetic field. The LSR describes the velocity frame in which the mean motion of the oldest stars in the Milky Way in the neighborhood of the Sun is zero, and is the reference frame in which cosmic rays assume near uniformity (in velocity direction). The local interstellar magnetic field direction from the IBEX ribbon center is within ~33°±20° of the magnetic field direction derived by interstellar polarization data from stars within 40 pc (*10*, *11*). Here, we show that the anisotropy maps of high-energy (TeV) cosmic rays likely provide independent confirmation of the interstellar magnetic field orientation inferred from the IBEX ribbon center.

The flux of high-energy (TeV) Galactic Cosmic Rays (GCRs) varies as a function of look direction in the sky. The large-scale structure in the TeV GCR sky consists of two broad asymmetries with flux variations of ~0.2%: a deficit of GCR flux at high galactic latitudes (the "loss-cone") and an excess of flux in the heliotail (*12*) direction [the "tail-in" excess (*13–21*)]. Small-scale TeV anisotropies (less than ~10°) in cosmic ray arrival directions possibly arise from cosmic ray propagation in a turbulent magnetic field (*22*). Because TeV GCRs have gyroradii of less than 700 AU (less than 0.005 parsec or pc; 1 pc = $3x10^{18}$ cm=200,000 AU) in the LISM, the observed GCR asymmetries must originate in the immediate interstellar environment of the Sun. This study extends and builds on increasing knowledge of the LISM magnetic field (*3*, *4*, *10*, *11*, *23*, *24*) and interstellar flow (*2*, *25–28*) to understand the origin of the large-scale high-energy (TeV) cosmic ray anisotropy, which has remained uncertain.

The observed cosmic ray anisotropy has a number of features that may reflect ordering both by the entry of cosmic rays into the heliosphere and by the interstellar magnetic field. It has been found (*13*) that the tail-in excess weakens above 10 TeV because of the relative sizes of the GCR gyroradius and heliotail. Data from underground detectors in both hemispheres has led to precise positions of the asymmetries (*14*). Additionally, the underground muon observatory Super-Kamiokande I obtained similar asymmetries for the 10 TeV GCR flux, with a deficit toward the constellation of Virgo representing the northern galactic deficit, and an excess in the direction of the heliotail, toward the constellation of Taurus (*15*). The direction of the Taurus excess is within 29° of the local interstellar magnetic field defined by the IBEX ribbon (Table 1), and within 23° from the local interstellar downwind direction (*1*). Milagro observations in the northern hemisphere (*19*) in combination with Ice Cube observations in the southern hemisphere (*20*) have confirmed that the galactic deficit is centered at high galactic latitudes and extends into both hemispheres (*21*). A global GCR anisotropy model constructed with unidirectional and bidirectional components and applied to results of the Tibet Asγ experiment attributed the bidirectional flow to GCRs drifting parallel to the local interstellar magnetic field.

The cosmic ray anisotropy, according to standard diffusion theory [e.g., (*29*, *30*)], is proportional to the average streaming of cosmic rays. Here, we take a small [0.3% (*31*)] ratio of perpendicular to parallel diffusion as well as an interstellar flow direction to be nearly perpendicular to the magnetic field based on IBEX observations. In this parameter regime, cosmic rays are largely guided by the interstellar magnetic field because both the anisotropic and perpendicular components of the anisotropy (fig. S1) are small compared to the field-aligned component.

We consider two scenarios for the formation of the cosmic ray anisotropy. In the first scenario, the magnitude of the anisotropy is determined in part by spatial gradients in the average cosmic ray density in response to the interstellar flow (eq. S6). For example, an outward plasma flow from the center of the LCC cluster (Fig. 1) pushes some cosmic

rays out of the local interstellar environment in which the heliosphere resides. This creates a spatial gradient in the cosmic ray density in the direction of the source and flow, which the average streaming (grey vector, Fig. 1) of cosmic rays tends to oppose.

The streaming direction of cosmic rays is determined on relatively small scales (on the scale of the cosmic ray gyroradii, less than 1% of a pc), whereas the streaming magnitude is determined over much larger scales of 10's of pc (*32*, *33*) controlled by the scattering (random-changes in direction) of cosmic rays caused by interactions with the turbulent interstellar magnetic field.

It is important to differentiate (*34*, *35*) between the interstellar magnetic field on local scales (~1000's AU or ~0.005-0.01 pc) and on larger (parsec) scales due to the presence of turbulence (*36–41*). Turbulence disrupts steady flows by random motion. In the interstellar medium, turbulent motion causes tangling and complexity in the structure of the interstellar magnetic field. The coherence scale length in the interstellar medium—the approximate distance along which the magnetic field appears relatively ordered—is typically 1-10 pc (*37*). Hence, the average magnetic field direction at these scales could be very different than in the vicinity of the heliosphere. At the large field-to-flow angle (87.6 ± 3.0°**)** found by IBEX (excepting the small region within 0.3° of exact perpendicularity where perpendicular diffusion dominates for the 0.3% ratio of perpendicular to parallel diffusion taken here), the cosmic ray density gradient becomes large so that the projection of the cosmic ray streaming into the flow plane opposes the interstellar velocity. The cosmic ray gradient in this case depends largely on the ratio of perpendicular to parallel diffusion. Reduced levels of perpendicular diffusion cause increased density gradients and thus stronger interstellar modulation of cosmic rays.

The ~0.2% high-energy (TeV) cosmic ray anisotropy suggests a magnitude for the ratio of perpendicular to parallel diffusion of only 0.3% (fig. S1). This ratio is compatible with recent results (*31*), but an order-of-magnitude smaller than the derived ~4% ratio of perpendicular-to-parallel diffusion (*41*) based on cosmic ray lifetimes in the galaxy (*39*). Simulations of cosmic ray diffusion (*42*) similarly predicted a ratio of perpendicular to parallel diffusion of ~2-4% at MeV-GeV energies, which are lower than the TeV energies considered here. The relatively small ratio of perpendicular to parallel diffusion of (~0.3%) may be a result of lower turbulence levels in the LIC compared to other portions of the galaxy.

In our second scenario for the cosmic ray anisotropy, we consider the contributions of supernova remnants (SNR) to the local cosmic ray gradient (*43–48*). A statistical model of cosmic rays originating from SNR sources based on the temporal and spatial distributions of supernova sources (*43*) suggests cosmic rays are injected locally by different sources and time-dependently diffuse throughout the galaxy. In the case of the convective anisotropy (supplementary text, section 2), the cosmic ray gradient is created by steady cosmic ray diffusion against the interstellar flow. Therefore the cosmic ray gradient driven by SNRs depends on the time and spatial distribution of SNR sources. Because parallel diffusion in the LISM is far more rapid than perpendicular diffusion, cosmic rays have a strong tendency to stream along the interstellar magnetic field. Provided that the GCR density gradient along the LISM magnetic field has the same sign as that of the convective gradient, and that the cosmic ray density gradient produces a maximum anisotropy magnitude similar to that in observations, the anisotropy associated with diffusion from SNR sources has a similar global morphology as the convective anisotropy (supplementary text, section 5). In other words, the dominance of parallel diffusion in the LISM can result in a similar global morphology for both the convective anisotropy and that driven by SNR sources.

We developed a model of the LISM magnetic field that is deflected around the heliosphere (supplementary text, section 3) and analyzed its influence on high-energy (TeV) cosmic ray anisotropies. We constructed a sky map (Fig. 2) of cosmic ray flux as viewed from the Sun using Monte-Carlo calculations of 10^4 individual cosmic ray trajectories in this perturbed magnetic field structure.

General ordering about the magnetic equator deduced from the IBEX ribbon is apparent in the high-energy (TeV) cosmic rays observations (Fig. 2, left). Some features absent in the simulation results can be attributed to the model's lack of interstellar turbulence (*22*) that should cause small-scale anisotropic structures and local GCR acceleration that may result in a more defined excess near the heliotail (*21*), and asymmetric influences on the heliosphere by the interstellar magnetic field (*49–53*). The modeled and observed anisotropies show some differences (e.g., the region from RA=-30° to 90° shows weaker modeled than observed anisotropies).

The fact that a similar ordering of the global cosmic ray anisotropy maps is generated simply by taking into account IBEX observations of low energy interstellar neutral atoms to deduce the interstellar velocity, and the IBEX ribbon to deduce the local interstellar magnetic field direction reveals consistency with independent observations across ten orders of magnitude in particle energy (keV energies in the IBEX ribbon compared to 10 TeV cosmic ray energies). Thus, local interstellar conditions play a key role in ordering very high-energy (TeV) cosmic rays in the immediate interstellar environment of the Sun.

References and Notes

1. N. A. Schwadron, H. E. Spence, R. Came, Does the space environment affect the ecosphere? *Eos* **92**, 297 (2011). doi:10.1029/2011EO360001
2. D. J. McComas, D. Alexashov, M. Bzowski, H. Fahr, J. Heerikhuisen, V. Izmodenov, M. A. Lee, E. Möbius, N. Pogorelov, N. A. Schwadron, G. P. Zank, The heliosphere's interstellar interaction: No bow shock. *Science* **336**, 1291–1293 (2012). Medline doi:10.1126/science.1221054
3. D. J. McComas, F. Allegrini, P. Bochsler, M. Bzowski, E. R. Christian, G. B. Crew, R. DeMajistre, H. Fahr, H. Fichtner, P. C. Frisch, H. O. Funsten, S. A. Fuselier, G. Gloeckler, M. Gruntman, J. Heerikhuisen, V. Izmodenov, P. Janzen, P. Knappenberger, S. Krimigis, H. Kucharek, M. Lee, G. Livadiotis, S. Livi, R. J. MacDowall, D. Mitchell, E. Möbius, T. Moore, N. V. Pogorelov, D. Reisenfeld, E. Roelof, L. Saul, N. A. Schwadron, P. W. Valek, R. Vanderspek, P. Wurz, G. P. Zank, Global observations of the interstellar interaction from the Interstellar Boundary Explorer (IBEX). *Science* **326**, 959–962 (2009). Medline doi:10.1126/science.1180906
4. N. A. Schwadron, M. Bzowski, G. B. Crew, M. Gruntman, H. Fahr, H. Fichtner, P. C. Frisch, H. O. Funsten, S. Fuselier, J. Heerikhuisen, V. Izmodenov, H. Kucharek, M. Lee, G. Livadiotis, D. J. McComas, E. Moebius, T. Moore, J. Mukherjee, N. V. Pogorelov, C. Prested, D. Reisenfeld, E. Roelof, G. P. Zank, Comparison of Interstellar Boundary Explorer observations with 3D global heliospheric models. *Science* **326**, 966–968 (2009). Medline doi:10.1126/science.1180986
5. H. O. Funsten, F. Allegrini, G. B. Crew, R. DeMajistre, P. C. Frisch, S. A. Fuselier, M. Gruntman, P. Janzen, D. J. McComas, E. Möbius, B. Randol, D. B. Reisenfeld, E. C. Roelof, N. A. Schwadron, Structures and spectral variations of the outer heliosphere in IBEX energetic neutral atom maps. *Science* **326**, 964–966 (2009). Medline doi:10.1126/science.1180927
6. S. A. Fuselier, F. Allegrini, H. O. Funsten, A. G. Ghielmetti, D. Heirtzler, H. Kucharek, O. W. Lennartsson, D. J. McComas, E. Möbius, T. E. Moore, S. M. Petrinec, L. A. Saul, J. A. Scheer, N. Schwadron, P. Wurz, Width and variation of the ENA flux ribbon observed by the Interstellar Boundary Explorer. *Science* **326**, 962–964 (2009). Medline doi:10.1126/science.1180981
7. J. Heerikhuisen, N. V. Pogorelov, G. P. Zank, G. B. Crew, P. C. Frisch, H. O. Funsten, P. H. Janzen, D. J. McComas, D. B. Reisenfeld, N. A. Schwadron, Pick-up ions in the outer heliosheath: A possible mechanism for the interstellar boundary EXplorer ribbon. *Astrophys. J.* **708**, L126–L130 (2010). doi:10.1088/2041-8205/708/2/L126
8. J. Heerikhuisen, N. V. Pogorelov, An estimate of the nearby interstellar magnetic field using neutral atoms. *Astrophys. J.* **738**, 29 (2011). doi:10.1088/0004-637X/738/1/29
9. N. A. Schwadron, D. J. McComas, Spatial retention of ions producing the *IBEX*

ribbon. *Astrophys. J.* **764**, 92 (2013). doi:10.1088/0004-637X/764/1/92
10. P. C. Frisch, B.-G. Andersson, A. Berdyugin, V. Piirola, R. DeMajistre, H. O. Funsten, A. M. Magalhaes, D. B. Seriacopi, D. J. McComas, N. A. Schwadron, J. D. Slavin, S. J. Wiktorowicz, The interstellar magnetic field close to the Sun. II. *Astrophys. J.* **760**, 106 (2012). doi:10.1088/0004-637X/760/2/106
11. P. C. Frisch, N. A. Schwadron, http://arxiv.org/abs/1310.2922 (2013).
12. D. J. McComas, M. A. Dayeh, H. O. Funsten, G. Livadiotis, N. A. Schwadron, The heliotail revealed by the *Interstellar Boundary Explorer*. *Astrophys. J.* **771**, 77 (2013). doi:10.1088/0004-637X/771/2/77
13. K. Nagashima, K. Fujimoto, R. M. Jacklyn, Galactic and heliotail-in anisotropies of cosmic rays as the origin of sidereal daily variation in the energy region < 10^4 GeV. *J. Geophys. Res.* **103**, 17429 (1998). doi:10.1029/98JA01105
14. D. L. Hall, K. Munakata, S. Yasue, S. Mori, C. Kato, M. Koyama, S. Akahane, Z. Fujii, K. Fujimoto, J. E. Humble, A. G. Fenton, K. B. Fenton, M. L. Duldig, Gaussian analysis of two hemisphere observations of galactic cosmic ray sidereal anisotropies. *J. Geophys. Res.* **104**, 6737 (1999). doi:10.1029/1998JA900107
15. G. Guillian, J. Hosaka, K. Ishihara, J. Kameda, Y. Koshio, A. Minamino, C. Mitsuda, M. Miura, S. Moriyama, M. Nakahata, T. Namba, Y. Obayashi, H. Ogawa, M. Shiozawa, Y. Suzuki, A. Takeda, Y. Takeuchi, S. Yamada, I. Higuchi, M. Ishitsuka, T. Kajita, K. Kaneyuki, G. Mitsuka, S. Nakayama, H. Nishino, A. Okada, K. Okumura, C. Saji, Y. Takenaga, S. Desai, E. Kearns, J. Stone, L. Sulak, W. Wang, M. Goldhaber, D. Casper, W. Gajewski, J. Griskevich, W. Kropp, D. Liu, S. Mine, M. Smy, H. Sobel, M. Vagins, K. Ganezer, J. Hill, W. Keig, K. Scholberg, C. Walter, R. Ellsworth, S. Tasaka, A. Kibayashi, J. Learned, S. Matsuno, M. Messier, Y. Hayato, A. Ichikawa, T. Ishida, T. Ishii, T. Iwashita, T. Kobayashi, T. Nakadaira, K. Nakamura, K. Nitta, Y. Oyama, Y. Totsuka, A. Suzuki, M. Hasegawa, I. Kato, H. Maesaka, T. Nakaya, K. Nishikawa, H. Sato, S. Yamamoto, M. Yokoyama, T. Haines, S. Dazeley, S. Hatakeyama, R. Svoboda, E. Blaufuss, J. Goodman, G. Sullivan, D. Turcan, A. Habig, Y. Fukuda, Y. Itow, M. Sakuda, M. Yoshida, S. Kim, J. Yoo, H. Okazawa, T. Ishizuka, C. Jung, T. Kato, K. Kobayashi, M. Malek, C. Mauger, C. McGrew, E. Sharkey, C. Yanagisawa, Y. Gando, T. Hasegawa, K. Inoue, J. Shirai, A. Suzuki, K. Nishijima, H. Ishino, Y. Watanabe, M. Koshiba, D. Kielczewska, H. Berns, R. Gran, K. Shiraishi, A. Stachyra, K. Washburn, R. Wilkes, K. Munakata, Observation of the anisotropy of 10 TeV primary cosmic ray nuclei flux with the Super-Kamiokande-I detector. *Phys. Rev. D Part. Fields Gravit. Cosmol.* **75**, 062003 (2007). doi:10.1103/PhysRevD.75.062003
16. M. Amenomori *et al*., in *Proceedings of the 9th Annual International Astrophysics Conference*, *AIP Conference Proceedings*, J. Le Roux, G. P. Zank, A. J. Coates, V. Florinski, Eds. (American Institute of Physics, College Park, MD, 2010), vol. 1302, p. 285
17. M. Amenomori, The Tibet ASγ Collaboration, Modeling of the high-energy galactic cosmic-ray anisotropy. *Astrophys. Space Sci. Trans.* **6**, 49–52 (2010). doi:10.5194/astra-6-49-2010
18. A. A. Abdo, B. Allen, T. Aune, D. Berley, E. Blaufuss, S. Casanova, C. Chen, B. L. Dingus, R. W. Ellsworth, L. Fleysher, R. Fleysher, M. M. Gonzalez, J. A. Goodman, C. M. Hoffman, P. H. Hüntemeyer, B. E. Kolterman, C. P. Lansdell, J. T. Linnemann, J. E. McEnery, A. I. Mincer, P. Nemethy, D. Noyes, J. Pretz, J. M. Ryan, P. M. Parkinson, A. Shoup, G. Sinnis, A. J. Smith, G. W. Sullivan, V. Vasileiou, G. P. Walker, D. A. Williams, G. B. Yodh; Milagro Collaboration, Discovery of localized regions of excess 10-TeV cosmic rays. *Phys. Rev. Lett.* **101**, 221101 (2008). Medline doi:10.1103/PhysRevLett.101.221101
19. A. A. Abdo, B. T. Allen, T. Aune, D. Berley, S. Casanova, C. Chen, B. L. Dingus, R. W. Ellsworth, L. Fleysher, R. Fleysher, M. M. Gonzalez, J. A. Goodman, C. M. Hoffman, B. Hopper, P. H. Hüntemeyer, B. E. Kolterman, C. P. Lansdell, J. T. Linnemann, J. E. McEnery, A. I. Mincer, P. Nemethy, D. Noyes, J. Pretz, J. M. Ryan, P. M. S. Parkinson, A. Shoup, G. Sinnis, A. J. Smith, G. W. Sullivan, V. Vasileiou, G. P. Walker, D. A. Williams, G. B. Yodh, The large-scale cosmic-ray anisotropy as observed with Milagro. *Astrophys. J.* **698**, 2121–2130 (2009). doi:10.1088/0004-637X/698/2/2121
20. R. Abbasi, Y. Abdou, T. Abu-Zayyad, J. Adams, J. A. Aguilar, M. Ahlers, D. Altmann, K. Andeen, J. Auffenberg, X. Bai, M. Baker, S. W. Barwick, R. Bay, J. L. B. Alba, K. Beattie, J. J. Beatty, S. Bechet, J. K. Becker, K.-H. Becker, M. L. Benabderrahmane, S. BenZvi, J. Berdermann, P. Berghaus, D. Berley, E. Bernardini, D. Bertrand, D. Z. Besson, D. Bindig, M. Bissok, E. Blaufuss, J. Blumenthal, D. J. Boersma, C. Bohm, D. Bose, S. Böser, O. Botner, A. M. Brown, S. Buitink, K. S. Caballero-Mora, M. Carson, D. Chirkin, B. Christy, J. Clem, F. Clevermann, S. Cohen, C. Colnard, D. F. Cowen, M. V. D'Agostino, M. Danninger, J. Daughhetee, J. C. Davis, C. De Clercq, L. Demirörs, T. Denger, O. Depaepe, F. Descamps, P. Desiati, G. de Vries-Uiterweerd, T. DeYoung, J. C. Díaz-Vélez, M. Dierckxsens, J. Dreyer, J. P. Dumm, R. Ehrlich, J. Eisch, R. W. Ellsworth, O. Engdegård, S. Euler, P. A. Evenson, O. Fadiran, A. R. Fazely, A. Fedynitch, J. Feintzeig, T. Feusels, K. Filimonov, C. Finley, T. Fischer-Wasels, M. M. Foerster, B. D. Fox, A. Franckowiak, R. Franke, T. K. Gaisser, J. Gallagher, L. Gerhardt, L. Gladstone, T. Glüsenkamp, A. Goldschmidt, J. A. Goodman, D. Gora, D. Grant, T. Griesel, A. Groß, S. Grullon, M. Gurtner, C. Ha, A. Hajismail, A. Hallgren, F. Halzen, K. Han, K. Hanson, D. Heinen, K. Helbing, P. Herquet, S. Hickford, G. C. Hill, K. D. Hoffman, A. Homeier, K. Hoshina, D. Hubert, W. Huelsnitz, J.-P. Hülß, P. O. Hulth, K. Hultqvist, S. Hussain, A. Ishihara, J. Jacobsen, G. S. Japaridze, H. Johansson, J. M. Joseph, K.-H. Kampert, A. Kappes, T. Karg, A. Karle, P. Kenny, J. Kiryluk, F. Kislat, S. R. Klein, J.-H. Köhne, G. Kohnen, H. Kolanoski, L. Köpke, S. Kopper, D. J. Koskinen, M. Kowalski, T. Kowarik, M. Krasberg, T. Krings, G. Kroll, N. Kurahashi, T. Kuwabara, M. Labare, S. Lafebre, K. Laihem, H. Landsman, M. J. Larson, R. Lauer, J. Lünemann, B. Madajczyk, J. Madsen, P. Majumdar, A. Marotta, R. Maruyama, K. Mase, H. S. Matis, K. Meagher, M. Merck, P. Mészáros, T. Meures, E. Middell, N. Milke, J. Miller, T. Montaruli, R. Morse, S. M. Movit, R. Nahnhauer, J. W. Nam, U. Naumann, P. Nießen, D. R. Nygren, S. Odrowski, A. Olivas, M. Olivo, A. O'Murchadha, M. Ono, S. Panknin, L. Paul, C. P. de los Heros, J. Petrovic, A. Piegsa, D. Pieloth, R. Porrata, J. Posselt, C. C. Price, P. B. Price, G. T. Przybylski, K. Rawlins, P. Redl, E. Resconi, W. Rhode, M. Ribordy, A. Rizzo, J. P. Rodrigues, P. Roth, F. Rothmaier, C. Rott, T. Ruhe, D. Rutledge, B. Ruzybayev, D. Ryckbosch, H.-G. Sander, M. Santander, S. Sarkar, K. Schatto, T. Schmidt, A. Schönwald, A. Schukraft, A. Schultes, O. Schulz, M. Schunck, D. Seckel, B. Semburg, S. H. Seo, Y. Sestayo, S. Seunarine, A. Silvestri, A. Slipak, G. M. Spiczak, C. Spiering, M. Stamatikos, T. Stanev, G. Stephens, T. Stezelberger, R. G. Stokstad, A. Stössl, S. Stoyanov, E. A. Strahler, T. Straszheim, M. Stür, G. W. Sullivan, Q. Swillens, H. Taavola, I. Taboada, A. Tamburro, A. Tepe, S. Ter-Antonyan, S. Tilav, P. A. Toale, S. Toscano, D. Tosi, D. Turčan, N. van Eijndhoven, J. Vandenbroucke, A. Van Overloop, J. van Santen, M. Vehring, M. Voge, C. Walck, T. Waldenmaier, M. Wallraff, M. Walter, C. Weaver, C. Wendt, S. Westerhoff, N. Whitehorn, K. Wiebe, C. H. Wiebusch, D. R. Williams, R. Wischnewski, H. Wissing, M. Wolf, T. R. Wood, K. Woschnagg, C. Xu, X. W. Xu, G. Yodh, S. Yoshida, P. Zarzhitsky, M. Zoll, Observation of anisotropy in the arrival directions of galactic cosmic rays at multiple angular scales with IceCube. *Astrophys. J.* **740**, 16 (2011). doi:10.1088/0004-637X/740/1/16
21. P. Desiati, A. Lazarian, Anisotropy of TeV cosmic rays and outer heliospheric boundaries. *Astrophys. J.* **762**, 44 (2013). doi:10.1088/0004-637X/762/1/44
22. G. Giacinti, G. Sigl, Local magnetic turbulence and TeV-PeV cosmic ray anisotropies. *Phys. Rev. Lett.* **109**, 071101 (2012). Medline doi:10.1103/PhysRevLett.109.071101
23. R. Lallement, E. Quémerais, J. L. Bertaux, S. Ferron, D. Koutroumpa, R. Pellinen, Deflection of the interstellar neutral hydrogen flow across the heliospheric interface. *Science* **307**, 1447–1449 (2005). Medline doi:10.1126/science.1107953
24. M. Opher, E. C. Stone, T. I. Gombosi, The orientation of the local interstellar magnetic field. *Science* **316**, 875–878 (2007). Medline doi:10.1126/science.1139480
25. M. Witte, Kinetic parameters of interstellar neutral helium. *Astron. Astrophys.* **426**, 835–844 (2004). doi:10.1051/0004-6361:20035956
26. E. Möbius, P. Bochsler, M. Bzowski, G. B. Crew, H. O. Funsten, S. A. Fuselier, A. Ghielmetti, D. Heirtzler, V. V. Izmodenov, M. Kubiak, H. Kucharek, M. A. Lee, T. Leonard, D. J. McComas, L. Petersen, L. Saul, J. A. Scheer, N. Schwadron, M. Witte, P. Wurz, Direct observations of interstellar H, He, and O by the Interstellar Boundary Explorer. *Science* **326**, 969–971 (2009). Medline doi:10.1126/science.1180971
27. E. Möbius, P. Bochsler, M. Bzowski, D. Heirtzler, M. A. Kubiak, H. Kucharek, M. A. Lee, T. Leonard, N. A. Schwadron, X. Wu, S. A. Fuselier, G. Crew, D. J. McComas, L. Petersen, L. Saul, D. Valovcin, R. Vanderspek, P. Wurz, Interstellar gas flow parameters derived from Interstellar Boundary

Explorer-Lo Observations in 2009 and 2010: Analytical analysis. *Astrophys. J. Suppl. Ser.* **198**, 11 (2012). doi:10.1088/0067-0049/198/2/11
28. M. Bzowski, M. A. Kubiak, E. Möbius, P. Bochsler, T. Leonard, D. Heirtzler, H. Kucharek, J. M. Sokół, M. Hłond, G. B. Crew, N. A. Schwadron, S. A. Fuselier, D. J. McComas, Neutral interstellar helium parameters based on IBEX-Lo observations and test particle calculations. *Astrophys. J. Suppl. Ser.* **198**, 12 (2012). doi:10.1088/0067-0049/198/2/12
29. L. J. Gleeson, W. I. Axford, Solar modulation of galactic cosmic rays. *Astrophys. J.* **154**, 1011 (1968). doi:10.1086/149822
30. M. A. Forman, L. J. Gleeson, Cosmic-ray streaming and anisotropies. *Astrophys. Space Sci.* **32**, 77–94 (1975). doi:10.1007/BF00646218
31. A. Shalchi, I. Büsching, A. Lazarian, R. Schlickeiser, Perpendicular diffusion of cosmic rays for a Goldreich-Sridhar spectrum. *Astrophys. J.* **725**, 2117–2127 (2010). doi:10.1088/0004-637X/725/2/2117
32. I. Büsching, M. S. Potgieter, The variability of the proton cosmic ray flux on the Sun's way around the galactic center. *Adv. Space Res.* **42**, 504–509 (2008). doi:10.1016/j.asr.2007.05.051
33. V. S. Ptuskin, I. V. Moskalenko, F. C. Jones, A. W. Strong, V. N. Zirakashvili, Dissipation of magnetohydrodynamic waves on energetic particles: Impact on interstellar turbulence and cosmic-ray transport. *Astrophys. J.* **642**, 902–916 (2006). doi:10.1086/501117
34. J. R. Jokipii, Astronomy. Our interstellar neighborhood. *Science* **307**, 1424–1425 (2005). 10.1126/science.1109701 Medline doi:10.1126/science.1109701
35. J. R. Jokipii, Planetary science. A local wiggle in the turbulent interstellar magnetic field. *Science* **316**, 839–840 (2007). 10.1126/science.1141628 Medline doi:10.1126/science.1141628
36. L. C. Lee, J. R. Jokipii, The irregularity spectrum in interstellar space. *Astrophys. J.* **206**, 735 (1976). doi:10.1086/154434
37. A. H. Minter, S. R. Spangler, Observation of turbulent fluctuations in the interstellar plasma density and magnetic field on spatial scales of 0.01 to 100 Parsecs. *Astrophys. J.* **458**, 194 (1996). doi:10.1086/176803
38. S. Chandrasekhar, G. Munch, The theory of the fluctuations in brightness of the Milky way. V. *Astrophys. J.* **115**, 103 (1952). doi:10.1086/145518
39. J. R. Jokipii, E. N. Parker, Cosmic-ray life and the stochastic nature of the galactic magnetic field. *Astrophys. J.* **155**, 799 (1969). doi:10.1086/149910
40. J. W. Armstrong, B. J. Rickett, S. R. Spangler, Electron density power spectrum in the local interstellar medium. *Astrophys. J.* **443**, 209 (1995). doi:10.1086/175515
41. J. R. Jokipii, in *Proceedings of the 2nd Guillermo Haro Conference*, J. Franco, A. Carraminana, Eds. (Cambridge Univ. Press, Cambridge, 1999), p. 70.
42. J. Giacalone, J. R. Jokipii, The transport of cosmic rays across a turbulent magnetic field. *Astrophys. J.* **520**, 204–214 (1999). doi:10.1086/307452
43. P. Blasi, E. Amato, Diffusive propagation of cosmic rays from supernova remnants in the Galaxy. II: Anisotropy. *J. Cosmol. Astropart. Phys.* **2012**, 011 (2012). doi:10.1088/1475-7516/2012/01/011
44. A. D. Erlykin, A. W. Wolfendale, The anisotropy of galactic cosmic rays as a product of stochastic supernova explosions. *Astropart. Phys.* **25**, 183–194 (2006). doi:10.1016/j.astropartphys.2006.01.003
45. I. Büsching, M. Pohl, R. Schlickeiser, Excess GeV radiation and cosmic ray origin. *Astron. Astrophys.* **377**, 1056 (2001). doi:10.1051/0004-6361:20011125
46. M. Pohl, D. Eichler, Understanding tev-band cosmic-ray anisotropy. *Astrophys. J.* **766**, 4 (2013). doi:10.1088/0004-637X/766/1/4
47. I. Busching, A. Kopp, M. Pohl, R. Schlickeiser, C. Perrot, I. Grenier, Cosmic-ray propagation properties for an origin in supernova remnants. *Astrophys. J.* **619**, 314–326 (2005). doi:10.1086/426537
48. C. Evoli, D. Gaggero, D. Grasso, L. Maccione, Common solution to the cosmic ray anisotropy and gradient problems. *Phys. Rev. Lett.* **108**, 211102 (2012). Medline doi:10.1103/PhysRevLett.108.211102
49. G. P. Zank, Interaction of the solar wind with the local interstellar medium: a theoretical perspective. *Space Sci. Rev.* **89**, 413–688 (1999). doi:10.1023/A:1005155601277
50. R. Ratkiewicz *et al*., *Astron. Astrophys.* **335**, 363 (1998).
51. N. V. Pogorelov, G. P. Zank, The direction of the neutral hydrogen velocity in the inner heliosphere as a possible interstellar magnetic field compass. *Astrophys. J.* **636**, L161–L164 (2006). doi:10.1086/500087
52. M. Opher, E. C. Stone, P. C. Liewer, The effects of a local interstellar magnetic field on *Voyager 1* and *2* observations. *Astrophys. J.* **640**, L71–L74 (2006). doi:10.1086/503251
53. N. V. Pogorelov, J. Heerikhuisen, G. P. Zank, S. N. Borovikov, Influence of the interstellar magnetic field and neutrals on the shape of the outer heliosphere. *Space Sci. Rev.* **143**, 31–42 (2009). doi:10.1007/s11214-008-9429-x
54. R. Schönrich, J. Binney, W. Dehnen, Local kinematics and the local standard of rest. *Mon. Not. R. Astron. Soc.* **403**, 1829–1833 (2010). doi:10.1111/j.1365-2966.2010.16253.x
55. H. O. Funsten, R. DeMajistre, P. C. Frisch, J. Heerikhuisen, D. M. Higdon, P. Janzen, B. A. Larsen, G. Livadiotis, D. J. McComas, E. Möbius, C. S. Reese, D. B. Reisenfeld, N. A. Schwadron, E. J. Zirnstein, Circularity of the *Interstellar Boundary Explorer* ribbon of enhanced energetic neutral atom (ENA) flux. *Astrophys. J.* **776**, 30 (2013). doi:10.1088/0004-637X/776/1/30
56. M. Wolleben, A new model for the Loop I (North Polar Spur) region. *Astrophys. J.* **664**, 349–356 (2007). doi:10.1086/518711
57. P. C. Frisch, L. Grodnicki, D. E. Welty, The velocity distribution of the nearest interstellar gas. *Astrophys. J.* **574**, 834–846 (2002). doi:10.1086/341001
58. J. L. Linsky, B. J. Rickett, S. Redfield, The origin of radio scintillation in the local interstellar medium. *Astrophys. J.* **675**, 413–419 (2008). doi:10.1086/526420
59. B. E. Wood, J. L. Linsky, G. P. Zank, Heliospheric, astrospheric, and interstellar Lyα absorption toward 36 Ophiuchi. *Astrophys. J.* **537**, 304–311 (2000). doi:10.1086/309026
60. R. Lallement *et al*., *Astron. Astrophys.* **286**, 898 (1994).
61. G. Hébrard *et al*., *Astron. Astrophys.* **350**, 643 (1999).
62. J. D. Slavin, P. C. Frisch, The boundary conditions of the heliosphere: Photoionization models constrained by interstellar and in situ data. *Astron. Astrophys.* **491**, 53–68 (2008). doi:10.1051/0004-6361:20078101
63. N. A. Schwadron, F. Allegrini, M. Bzowski, E. R. Christian, G. B. Crew, M. Dayeh, R. DeMajistre, P. Frisch, H. O. Funsten, S. A. Fuselier, K. Goodrich, M. Gruntman, P. Janzen, H. Kucharek, G. Livadiotis, D. J. McComas, E. Moebius, C. Prested, D. Reisenfeld, M. Reno, E. Roelof, J. Siegel, R. Vanderspek, Separation of the *Interstellar Boundary Explorer* ribbon from globally distributed energetic neutral atom flux. *Astrophys. J.* **731**, 56 (2011). doi:10.1088/0004-637X/731/1/56
64. S. Redfield, J. L. Linsky, The structure of the local interstellar medium. IV. Dynamics, morphology, physical properties, and implications of cloud-cloud interactions. *Astrophys. J.* **673**, 283–314 (2008). doi:10.1086/524002
65. A. W. Strong, I. V. Moskalenko, V. S. Ptuskin, Cosmic-ray propagation and interactions in the Galaxy. *Annu. Rev. Nucl. Part. Sci.* **57**, 285–327 (2007). doi:10.1146/annurev.nucl.57.090506.123011
66. M. Abramowitz, I. A. Stegun, *Handbook of Mathematical Functions* (Dover, New York, 1970).
67. M. A. Mushref, Fourier-Bessel expansions with arbitrary radial boundaries. *Appl. Math.* **1**, 18–23 (2010). doi:10.4236/am.2010.11003

Acknowledgments: We thank all those who made IBEX possible. IBEX is primarily funded by NASA's Explorers Program (Contract No. NNG05EC85C). IBEX data are available at http://ibex.swri.edu/researchers/publicdata.shtml. IceCube cosmic ray data are available from http://icecube.wisc.edu/science/data.

Supplementary Materials
www.sciencemag.org/cgi/content/full/science.1245026/DC1
Supplementary Text
Figs. S1 to S5
References (*56*–*67*)

21 August 2013; accepted 29 January 2014
Published online 13 February 2014
10.1126/science.1245026

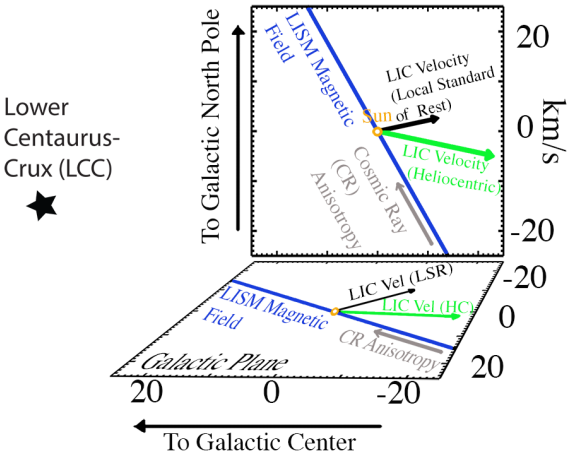

Fig. 1. LIC velocities and LISM magnetic field directions. The LIC velocities inferred from IBEX (2) in the heliocentric (HC; green vector) rest frame and the local standard of rest (LSR; black vector) in the galaxy. These vectors are shown in both the galactic plane (lower plane) and the plane containing the galactic poles (upper plane) relative to the magnetic field of the local interstellar medium (LISM; blue lines). The LIC velocity and magnetic field are a part of the Loop I superbubble roughly centered on the Lower Centaurus Crux subgroup of the Scorpius-Centaurus Association. The cosmic ray anisotropy (grey vector) indicates average streaming of cosmic rays.

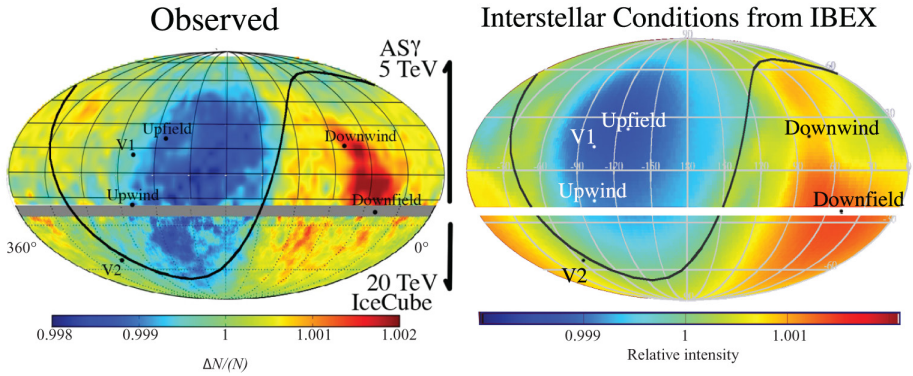

Fig. 2. TeV cosmic ray anisotropies compared with predictions. Comparison between observed (left) and modeled (right) cosmic ray relative intensities across the sky (J2000 coordinates). Black curves show the magnetic equator with a magnetic field direction derived from the center of the IBEX ribbon. On the left, the region below 25° S latitude is the anisotropy map from IceCube with a median energy of 20 TeV (*18*) and above 20° S latitude is the anisotropy map from ASγ with 5 TeV median energy (*15*). Similarly, the modeled map (right) at 20 TeV is shown below 25° S latitude and at 5 TeV above 20° S latitude. Both portions of the maps are smoothed over 3°-5° . Labels indicate upwind and downwind directions (*2*), the current locations of Voyager 1 (V1) and Voyager 2 (V2) directions, and the “upfield” and “downfield” directions. Downfield is along the LISM magnetic field determined by IBEX in the direction closest to the interstellar velocity and upfield is in the opposite direction. Plots are in equatorial coordinates with 0 hours at the right, and increasing longitudes toward the left.

Table 1.

	Magnitude (km/s)	Galactic Long. (°)	Galactic Lat. (°)	Equatorial Right Ascension. (°)	Equatorial Declination (°)
LISM flow velocity* (HC frame)	23.2 ± 0.3	185.25 ± 0.24	-12.0 ± 0.5	78.5 ± 0.6	18.0 ± 0.5
LISM flow velocity (LSR frame**)	18.0 ± 0.9	47.9 ± 2.9	23.8 ± 2.0	267.0 ± 3.0	23.2 ± 3.1
Interstellar Magnetic Field***		210.5 ± 2.6	-57.1 ± 1.0	48.5 ± 1.5	-21.2 ± 1.6

*Heliocentric (HC) rest frame (*1*)
**Heliocentric velocities are converted to the Local Standard of Rest (LSR) using the solar apex motion in (*54*).
***Field directions and uncertainty inferred from the IBEX highest energy steps (1.79 keV and 2.73 keV; (*55*)) in which the ribbon maintains coherence and has the largest Line-of-Sight.